

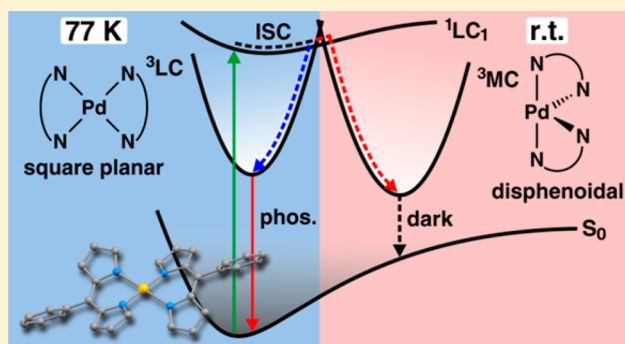
## Photoinduced Dynamics of Bis-dipyrinato-palladium(II) and Porphodimethenato-palladium(II) Complexes: Governing Near Infrared Phosphorescence by Structural Restriction

Stefan Riese, Marco Holzapfel, Alexander Schmiedel, Ingo Gert, David Schmidt, Frank Würthner,<sup>1</sup> and Christoph Lambert\*<sup>1</sup>

Institute of Organic Chemistry, Center for Nanosystems Chemistry, Universität Würzburg Am Hubland, D-97074 Würzburg, Germany

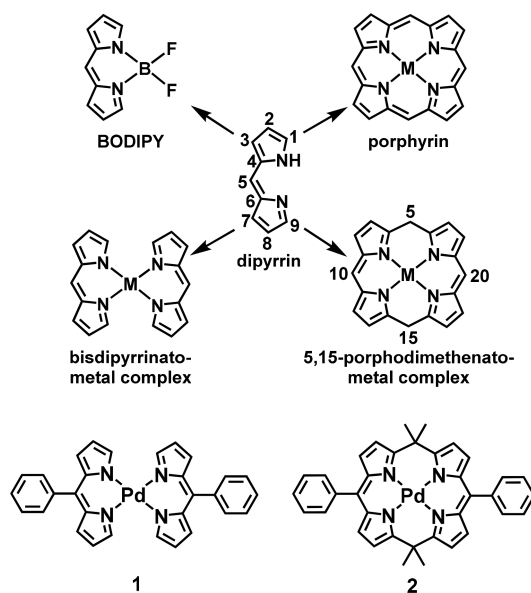
### Supporting Information

**ABSTRACT:** Although superficially similar, the bis-dipyrinato-palladium(II) complex **1** and the bridged porphodimethenato-palladium(II) complex **2** possess dramatically different structures in the ground state (proved by X-ray structure analysis) and in the singlet and triplet excited states (calculated by density functional theory methods). While complex **2** is rather rigid, complex **1** undergoes a major structural reorganization in the excited state to yield a disphenoidal (seesaw) triplet state. The dynamics of the excited states were probed by transient absorption spectroscopy with femtosecond and nanosecond time resolution and with fluorescence upconversion and yield intersystem crossing rate constants of ca.  $(13\text{--}16\text{ ps})^{-1}$ . The observation of significant near infrared phosphorescence in complex **2** but the absence of any emission in complex **1** in fluid solution could be rationalized by the structural reorganization of **1** which results in a nonemissive triplet metal centered state.



The observation of significant near infrared phosphorescence in complex **2** but the absence of any emission in complex **1** in fluid solution could be rationalized by the structural reorganization of **1** which results in a nonemissive triplet metal centered state.

Scheme 1. Dipyrryn Derivatives and Target Compounds **1** and **2**



### INTRODUCTION

Dipyrryn is a ligand that, attached to boron difluoride, forms the well-known BODIPY dyes which are widely used as strongly fluorescent chromophores.<sup>1–4</sup> However, dipyrryn is also known as a ligand to transition metals, also in form of homoleptic bis-dipyrinato metal complexes. Bridging the two dipyrryn ligands leads to partially saturated porphodimethenes and, after formal oxidation, to metalloporphyrins.<sup>5–8</sup> While, because of the aromatic nature of the fully conjugated porphyrin ring, the latter show electronic properties distinctly different from the former, the dipyrinato metal complexes are all characterized by a strong absorption around  $20\,000\text{ cm}^{-1}$  which is polarized along the long dipyrryn axis. However, the metal atom as well as specific groups attached to the *meso*-position of the dipyrryn ligand may change the photophysical behavior considerably, particularly concerning the lifetime of excited states.<sup>9</sup> While dipyrinato metal complexes with lighter transition metals and some main group metals have thoroughly been investigated concerning their photophysical properties,<sup>10–16</sup> not much is known about homo-<sup>6,17–19</sup> and heteroleptic<sup>6,17,20–26</sup> complexes of heavy transition metals with dipyrryn ligands. This is quite unfortunate because these complexes may be of potential use as near infrared (NIR) triplet emitters.

Received: April 13, 2018

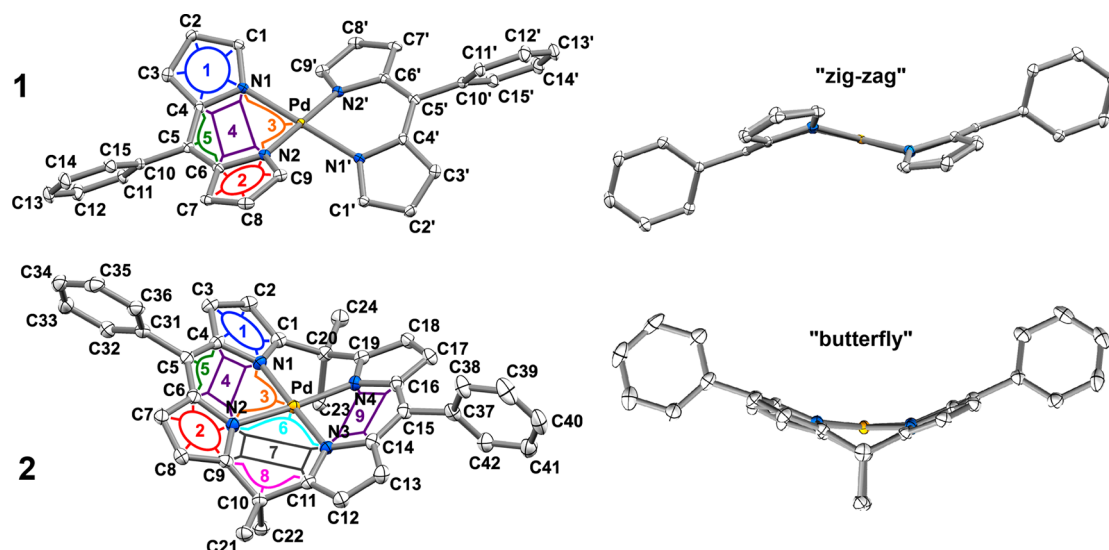


**Figure 1.** X-ray crystal structure of complexes **1** and **2**. Hydrogen atoms are removed for clarity. For **1**, only one-half of the asymmetric cell is shown. Thermal ellipsoids are at 50% probability level.

In particular, little is known about dipyrinato-palladium complexes.<sup>23</sup> Therefore, in this study, we focus on the photoinduced processes in bis-5-phenyldipyrrinato-palladium(II) **1** and 5,5',15,15'-tetramethyl-10,20-diphenylporphodimethenato-palladium(II) **2** (see Scheme 1), which may be considered as parent compounds to other more complex structures. Although complex **2** was prepared before by Lindsey et al.,<sup>27,28</sup> its photophysics has not yet been investigated. While complex **1** itself has not been reported until now, a few comparable bis-dipyrrinato-Pd(II) complexes were synthesized and reported to be practically nonemissive, except for a triarylamine-substituted derivative, which has a quantum yield of 1.5% and a fluorescence lifetime of 3.5 ns.<sup>18,19,29,30</sup> In the following, we first concentrate on structural aspects of the two complexes and then on their steady-state and time-resolved optical spectroscopic properties.

## RESULTS

**Structure.** Compound **2** was synthesized as previously described by Lindsey et al.<sup>28</sup> The synthesis of compound **1** is based on procedures described in the literature for similar Pd(II) complexes.<sup>18,29,30</sup> A detailed description of the synthetic protocols and the analytical data can be found in the Supporting Information.

The structures of **1** and **2** in the solid state were determined by X-ray crystal analysis and are depicted in Figure 1. Selected dihedral angles and distances can be found in the Supporting Information, Table S3. Compound **1** has an asymmetric unit cell comprised of two molecules with slightly different geometries. Because the differences between the two are small (on the order of 0.5° for dihedral angles and 0.01 Å for distances) and likely due to crystal packing forces, we discuss only the structural features of one molecule. Additional views of **1** and **2** depicting the complete unit cells are given in the Supporting Information, Figure S5. In the centrosymmetric ( $C_i$ ) compound **1**, the palladium possesses a square planar coordination sphere with Pd–N distances of ca. 2.01 Å. The two dipyrin ligands are highly bent (145.9° dihedral angle between planes 1 and 2) and tilted relative to the  $N_4$ Pd plane (148.4° dihedral angle between planes 3 and 4) forming a “zig-

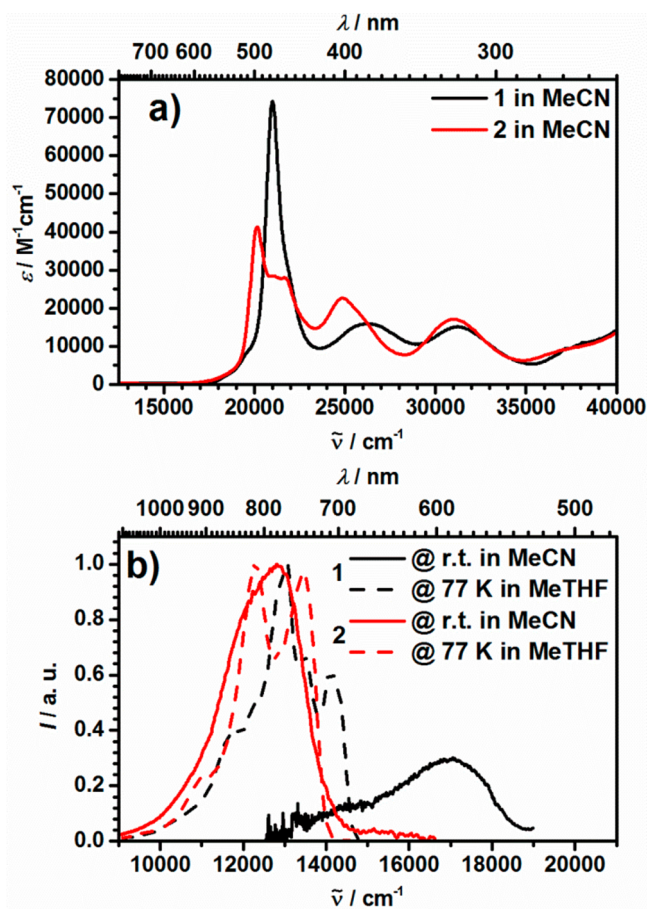


**Figure 2.** (a) Absorption spectra of **1** and **2** in MeCN. (b) Emission spectra of **1** and **2** in fluid MeCN at rt and frozen (77 K) MeTHF.

zag” geometry as to avoid steric repulsion of the C1/C9 hydrogen atoms with those at C9'/C1'.

In **2**, the palladium has a slightly distorted square planar coordination sphere with Pd–N distances of 2.00–2.01 Å. Furthermore, the dipyrin chromophores in **2** are almost planar (171.0° dihedral angle between planes 1 and 2), but the short

Table 1. Steady-State and Time Resolved Optical Spectroscopic Data of 1 and 2 in MeCN at rt

	${}^1\text{LC}_2 \tilde{\nu}_{\text{max}}/\text{cm}^{-1}$ ( $\epsilon_{\text{max}}/\text{M}^{-1} \text{cm}^{-1}$ )	${}^1\text{MLCT} \tilde{\nu}_{\text{max}}/\text{cm}^{-1}$ ( $\epsilon_{\text{max}}/\text{M}^{-1} \text{cm}^{-1}$ )	$\tilde{\nu}_{\text{em}}/\text{cm}^{-1}$	$\Phi_{\text{em}}$	fs-TA $\tau/\text{ps}$	fs-FLUC $t/\text{ps}$ (ampl.)	ns-TA $\tau/\text{ns}$
1	20 990 (74 300)	26 110 (15 800)	17 100	0.008		0.3 (0.43)	
					2.2	3.0 (0.28)	
					14	13 (0.29)	
2	20 160 (41 200)	24 860 (22 600)	12 800	0.008	inf.	0.1 (0.92)	53
					16	1 (0.08)	
					48	129 (0.003)	
					inf.		$81 \times 10^3$

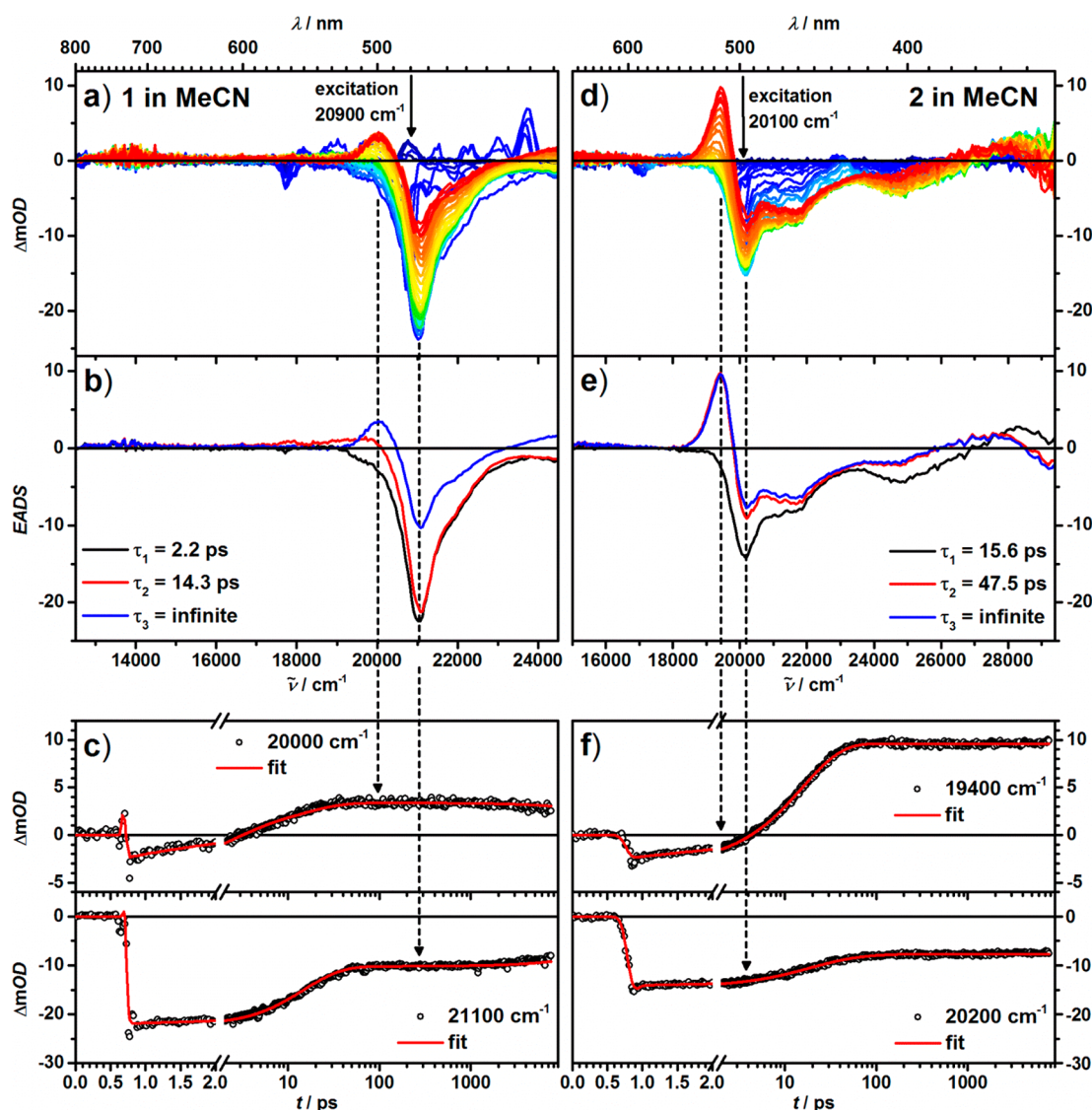


Figure 3. Chirp corrected transient absorption spectra of 1 and 2 in MeCN at rt (a and d), EADS from a global deconvolution (b and e), and time traces at selected wavenumbers with fit (c and f).

dimethylmethylene bridges between the two dipyrin subunits enforce butterfly (roof-top) geometry of the complex in which the two dipyrin chromophores possess a  $134.4^\circ$  dihedral angle (plane 4 and 9) relative to each other.<sup>31</sup>

**Steady-State Optical Spectroscopy.** Absorption spectra of both complexes were measured in MeCN at rt and are displayed in Figure 2a. Selected optical spectroscopic data are given in Table 1.

Both complexes show a strong absorption band at ca.  $20\,000 \text{ cm}^{-1}$  which is caused by a ligand centered (LC) transition, termed  ${}^1\text{LC}_2$  hereafter.<sup>18,23,32</sup> To the lower energy side, a much weaker band is visible as a shoulder, which we call  ${}^1\text{LC}_1$  in the following. These two bands can be interpreted as being caused by exciton coupling of the localized dipyrin LC transitions, which are polarized along the long axis of the dipyrin ligand. Accordingly, these two localized transition moments are face to face, which leads to an H-aggregate-like exciton splitting where

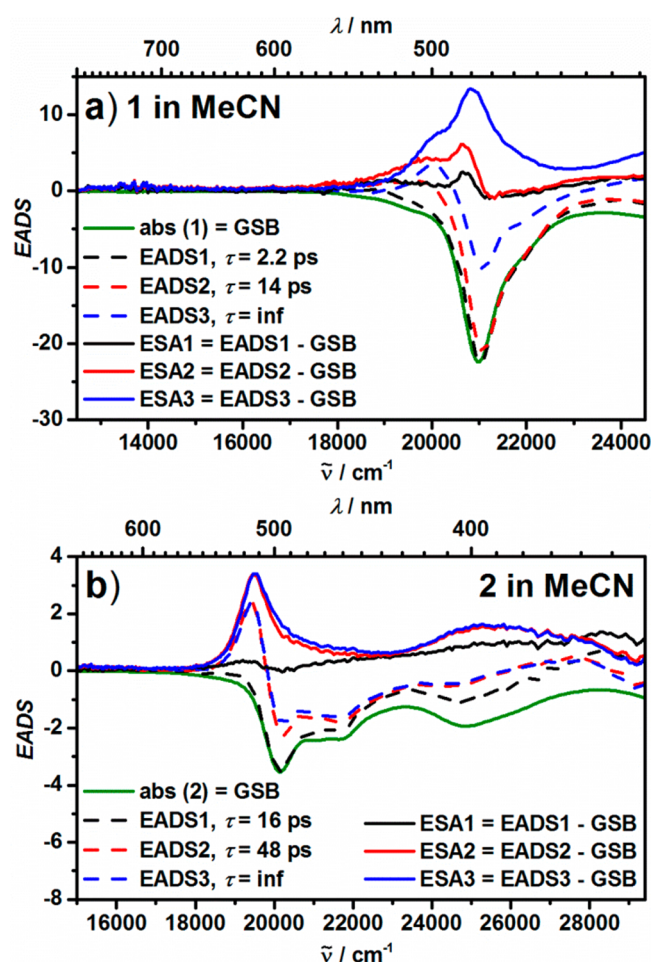


Figure 4. ESA from difference spectra of EADS and steady-state absorption spectra of **1** (a) and **2** (b) in MeCN.

the upper state is strongly allowed but the lower state is forbidden.<sup>11,18,32,33</sup> Furthermore, at ca. 25 000–26 000  $\text{cm}^{-1}$ , there is a pronounced MLCT band visible.<sup>23,34</sup>

At 77 K in frozen 2-MeTHF, both complexes show strong and vibrationally resolved phosphorescence between ca. 14 500 and 9000  $\text{cm}^{-1}$  (see Figure 2b), which is distinctly red-shifted compared to those recently reported for two phenylpyridyl-dipyrrin-palladium complexes.<sup>23</sup> This situation changes dramatically at rt in fluid MeCN. Here, the nonbridged dipyrin complex **1** emits a weak and unstructured fluorescence between 13 000 and 19 000  $\text{cm}^{-1}$  but no phosphorescence. In contrast, the bridged complex **2** shows relatively strong but unresolved phosphorescence with a quantum yield of 0.01 in MeCN (0.02 in THF) at the same spectral position as at 77 K, but no fluorescence.

**Time Resolved Optical Spectroscopy.** To obtain information about the photoinduced dynamics of complexes **1** and **2**, we performed transient absorption spectroscopy with femtosecond and nanosecond time resolution in fluid MeCN at rt.

In the femtosecond experiments, solutions of **1** or **2** in MeCN were excited with laser pulses (<150 fs, 1 kHz, generated using an OPA pumped with the amplified output of a Ti:sapphire laser at 800 nm) at the maximum of their  $^1\text{LC}_2$  band. The excited states were probed by a white light continuum, which was delayed by a controlled stage equipped with a retroreflector. The pump and probe beam met in a

quartz cell with 2 mm optical path length under magic angle. The instrument response was determined by fitting the coherent artifact to be ca. 180 fs (for details, see the Supporting Information).

The transient absorption (TA) spectra of **1** and **2** are displayed in Figure 3 in the top panels. We analyzed the TA data by a global deconvolution which uses the minimum number of exponential functions to produce evolution associated difference spectra (EADS) in a sequential model with increasing lifetimes. These EADS are given in the middle panels. In the bottom panels, time traces and the global fit for selected wavenumbers are superimposed.

As can be seen from the global analysis, there are three EADS for both complexes. Two of those possess lifetimes in the 2–50 ps time range, while the third one shows an infinite lifetime within the time window (8 ns) accessible with our instrumental setup.

In general, TA spectra may consist of ground state bleaching (GSB), stimulated emission (SE), and excited state absorption (ESA). Thus, we used the three EADS and subtracted the steady-state absorption spectrum, which yields the ESA contribution to each of the three EADS. The SE contribution is neglected here. As can be seen from Figure 4a for EADS1 of complex **1**, this subtraction gives an ESA1 with little structure because the EADS1 and the GSB (= negative steady state absorption spectrum) match very well. However, for the components ESA2 and ESA3 with longer lifetimes, there is pronounced amplitude visible at 21 000  $\text{cm}^{-1}$ . Furthermore, the absence of negative amplitudes at the low energy site of the GSB in the ESA indicates that there is no SE contribution. Compound **2** behaves very similarly; that is, the EADS1 matches very well with the steady-state absorption spectrum, but the EADS associated with longer lifetimes show a strong ESA contribution at ca. 19 500  $\text{cm}^{-1}$ .

The infinite lifetime of EADS3 shows for both complexes that a distinctly long-lived component contributes to the TA spectra. Therefore, we performed nanosecond laser flash spectroscopy with solutions of **1** and **2** in MeCN, which allows covering transient species down to the millisecond time regime. Thus, excitation at the  $^1\text{LC}_2$  band shows the immediate rise of a transient signal which matches excellently with the longest lived EADS from the femtosecond TA analysis (see Figure 5), that is, a strong GSB at 21 000  $\text{cm}^{-1}$  for **1** and at ca. 20 000/22 000  $\text{cm}^{-1}$  for **2**, associated with a strong ESA at lower wavenumbers for both complexes. Fits at selected wavenumbers yield monoexponential decays with  $\tau = 53$  ns for **1** and 81  $\mu\text{s}$  for **2**.

To complement the femtosecond transient absorption data and gain information about intersystem crossing (ISC) processes, we also performed fluorescence upconversion measurements (FLUC) at 25 000  $\text{cm}^{-1}$  excitation from the frequency doubled 800 nm output of the Ti:sapphire oscillator at 80 MHz. The fluorescence decays and their fit using several exponential functions convoluted with the instrument response are given in Figure 6. While complex **2** shows a decay with ca. 0.1 ps as the dominating component, complex **1** clearly displays multiexponential decay with three almost equally contributing components. The two longer time constants (3 and 13 ps) agree very well with those of the EADS of the TA measurements (2.2 and 14 ps). The time-resolved data from the femto- and nanosecond TA as well as the femtosecond FLUC measurements are collected in Table 1.

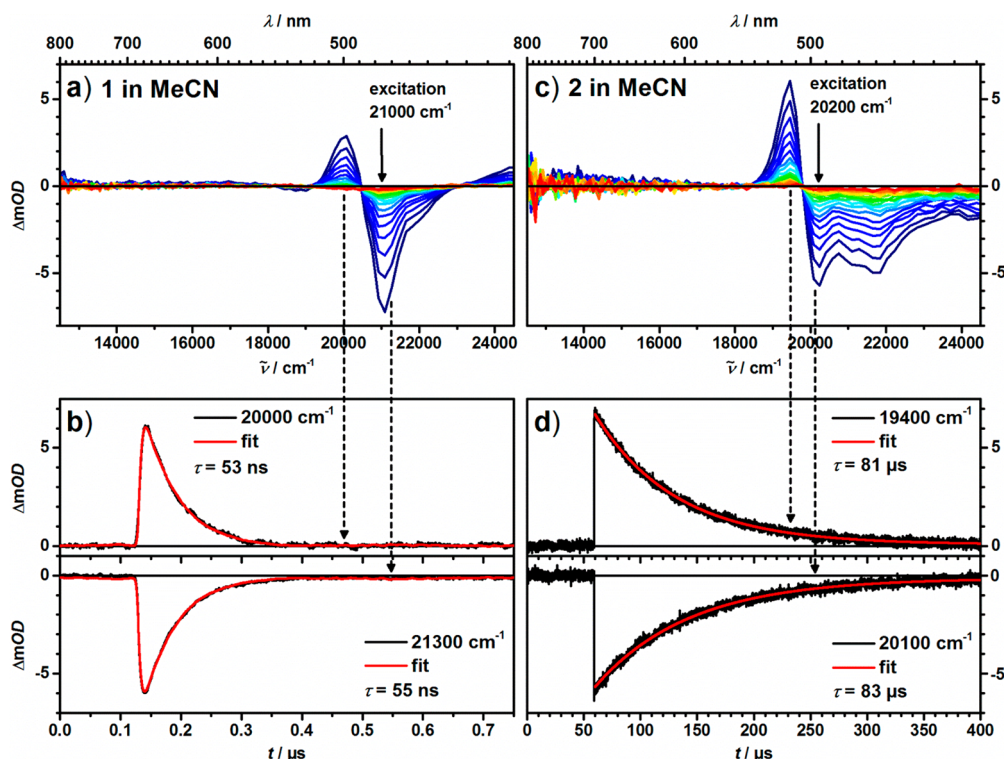


Figure 5. Nanosecond transient absorption spectra of 1 and 2 in MeCN at rt (a and c) and selected time traces with monoexponential fit (b and d).

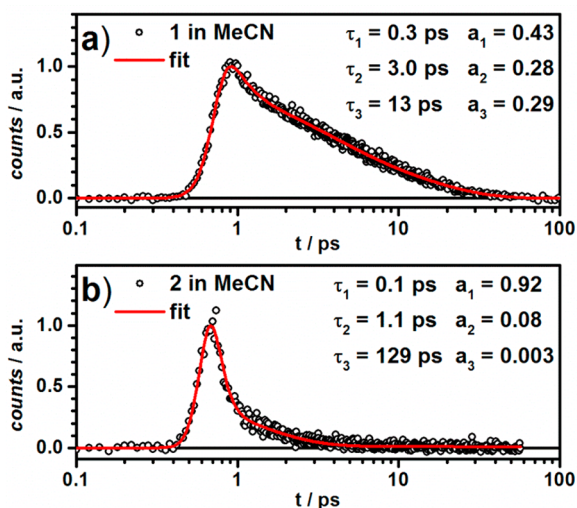


Figure 6. Fluorescence decay from fluorescence upconversion measurements of (a) 1 and (b) 2 in MeCN at rt at 25 000  $cm^{-1}$  excitation. The fluorescence was gated at 17 200  $cm^{-1}$  (IRF 0.24 ps) for 1 and at 18 700  $cm^{-1}$  (IRF 0.17 ps) for 2.

**Density Functional Theory (DFT) Computations.** To gain insight into structural and electronic aspects of the excited states of complexes 1 and 2, we performed DFT and time-dependent TD-DFT computations. Optimization of the ground states of 1 and 2 using the PBE1PBE functional and SDD-6-31G\* basis set combination shows excellent agreement with the X-ray crystal structure data; for a comparison of structural data, see Supporting Information, Table S3. For 1, we also found a ground state structure with  $D_2$  symmetry in which the palladium possesses a distorted tetrahedral coordination sphere. However, this structure is about 1600  $cm^{-1}$  higher in energy than the  $C_1$  symmetric structure, which corresponds to the experimental crystal structure. On the other hand, for 2, only one ground state structure with  $C_s$  symmetry was found. Based on these DFT optimized ground state structures with minimal energy ( $C_1$  for 1 and  $C_s$  for 2), we computed the vertical excitations into the LC states by the TD-DFT method. As anticipated above, the lowest excited  ${}^1LC_1$  state is forbidden in both complexes, but  ${}^1LC_2$  is allowed (see Table 2). This is the consequence of a symmetric ( $A_g$  for 1 and  $A''$  for 2) and antisymmetric ( $A_u$  for 1 and  $A'$  for 2) combination of dipyrin transition moments. The absolute energies of these computed transitions into  ${}^1LC_2$  are by ca. 1500  $cm^{-1}$  too high compared to the experimental energies (see Table 1). However, the

Table 2. DFT Calculated Energies ( $cm^{-1}$ ), Oscillator Strength ( $f$ ), and Symmetry of Franck–Condon (FC) and Optimized Excited States (TD-DFT for Singlet and UDFT for Triplet States)

	${}^1LC_1(FC)$ ( $f$ )	${}^1LC_2(FC)$ ( $f$ )	${}^1LC_1$	${}^1LC_1$	${}^1LC_1$	${}^3LC$	${}^3LC$	${}^3MC$
1	21 737 (0.0000) ( $C_1$ )	22 918 (0.0176) ( $C_1$ )	24 037 <sup>a</sup> ( $D_2$ )	20 767 <sup>a</sup> ( $C_1$ )	19 272 ( $C_1$ )	19 268 ( $D_2$ )	16 692 ( $C_1$ )	12 567 (disph, $\sim C_2$ )
2	20 008 (0.0006) ( $C_s$ )	21 640 (0.0270) ( $C_s$ )			18 405 ( $\sim C_s$ )		14 616 ( $\sim C_s$ )	

<sup>a</sup>Transition state.

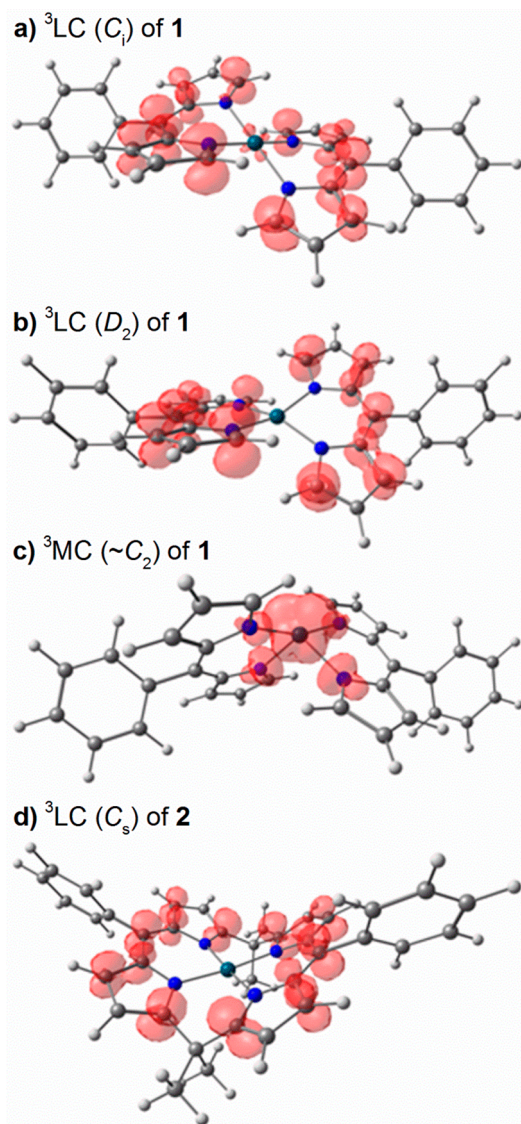


**Figure 7.** UDFT calculated geometries and spin densities of excited triplet states of **1** and **2**.

splitting  $\Delta E = 1180 \text{ cm}^{-1}$  (**1**) and  $1632 \text{ cm}^{-1}$  (**2**) of the two transitions which corresponds to twice the exciton coupling energy appears to be reasonable when compared to the difference of the experimental 00-energies of  $^1\text{LC}_1$  and  $^1\text{LC}_2$  from Figure 8 ( $1500 \text{ cm}^{-1}$  (**1**) and  $1600 \text{ cm}^{-1}$  (**2**)).

We also optimized the lowest lying excited states of **1** and **2** using two different strategies. The singlet  $^1\text{LC}_1$  state of **1** was optimized by TD-DFT, which gave a structure very similar to the ground state structure. Optimized in  $C_i$  symmetry, this structure turned out to be a transition state by frequency analysis but a distorted structure ( $C_i$ ) is a minimum on the excited state hypersurface. While the four Pd–N distances in this symmetry-broken singlet structure vary slightly ( $1.991$  and  $1.974 \text{ \AA}$  to one dipyrin ligand and  $2.071$  and  $2.070 \text{ \AA}$  to the other), the strongest differences to the ground state structure refer to the dihedral angles between planes 3/4 ( $= \theta_{3/4}$ ). This angle is  $157.2^\circ$  in the singlet excited state which deviates somewhat from that of the DFT optimized ground state ( $\theta_{3/4} = 149.0^\circ$ ) and the experimental crystal structure ( $\theta_{3/4} = 148.4^\circ$ ). Another singlet  $^1\text{LC}_1$  state with exact  $D_2$  symmetry and distorted tetrahedral coordination sphere of Pd (which refers to

the computed  $D_2$  ground state structure) also turned out to be transition states by frequency analysis.

For the corresponding triplet states, we used the UDFT method. Engels et al.<sup>35</sup> recently showed that using this strategy yields reasonable singlet–triplet energy differences. Here, we found three different minimum structures: one with  $C_i$  symmetry which corresponds to the crystal structure with square planar coordinated palladium and bent dipyrin ligands (see Figure 7a), a second one in which the palladium has a strongly distorted tetrahedral coordination sphere ( $D_2$ ) with planar dipyrin ligands (see Figure 7b), and a third, where the palladium possesses a disphenoidal (seesaw) coordination sphere ( $\sim C_2$ ) and planar ligands (Figure 7c). For the  $D_2$  and the  $\sim C_2$  triplet structures, we did not find any corresponding minimum singlet excited state structures, but transition states. Clearly, the disphenoidal structure is the lowest energy triplet structure (see Table 2). In this structure, the spin density is localized at the palladium atom (see Figure 7c), which also leads to an elongation of the Pd–N bonds which are  $2.102$  and  $2.114 \text{ \AA}$ . Thus, the disphenoidal triplet state can be viewed as a metal centered  $^3\text{MC}$  state. While usually a square planar coordination sphere predominates for Pd(II) complexes in the ground state, some exceptions are known, which include tetrahedral,<sup>36</sup> trigonal pyramidal,<sup>37</sup> and disphenoidal<sup>38</sup> structures. For the tetrahedral structure, a triplet state was rationalized based on magnetic measurements which show that deviations from square planar geometry can indeed be preferred for open-shell Pd(II) species as is the triplet MC state here.<sup>36</sup>

The other two triplet states of **1** have distinctly higher energy, and the spin density is delocalized over the dipyrin ligands with little, if at all, participation of the metal atom.

Much in contrast to **1**, for **2**, besides a nearly symmetric  $^1\text{LC}_1$  state ( $\sim C_s$ ) whose butterfly geometry is even stronger folded than in the ground state ( $\theta_{4/9} = 120.3^\circ$  ( $^1\text{LC}_1$ ) vs  $133.9^\circ$  ( $S_0$ )), we found only one excited triplet state which has a similar geometry as the  $^1\text{LC}_1$  state ( $\sim C_s$ ,  $d_{\text{Pd-N}} = 1.995$  and  $2.006 \text{ \AA}$ ;  $\theta_{4/9} = 123.3^\circ$ ). Here, the spin density is delocalized over the two dipyrin ligands (see Figure 7d). The relative energies of all these states are collected in Table 2.

## DISCUSSION AND CONCLUSION

With the spectroscopic and computational information at hand, we can construct a state diagram for the photophysical processes in complexes **1** and **2** which are sketched in Figure 8. In these diagrams, the corresponding 00-energies of states were estimated from the intersection of the energy axis with tangents drawn at the low energy side of absorption or high energy side of emission spectra.

Fluorescence decays as measured by FLUC at a single wavenumber give a first hint about the early photoinduced dynamics involving both  $^1\text{LC}_2$  and  $^1\text{LC}_1$  states because the fluorescence from these states is expected to be broad and strongly overlapping. For complex **1**, excitation into the intense  $^1\text{LC}_2$  band populates a very short-lived singlet state whose existence cannot be proved by TA spectroscopy but is evident by the  $300 \text{ fs}$  time constant of the fluorescence decay in the FLUC measurement. This time constant refers to the internal conversion to the  $^1\text{LC}_1$  state which is visible in the TA spectra as an EADS which consists of almost pure GSB. The fact that the  $^1\text{LC}_2$  state is not visible in the TA spectra is probably caused by the fact that it is very short-lived and consists almost purely of GSB and therefore cannot be distinguished from the

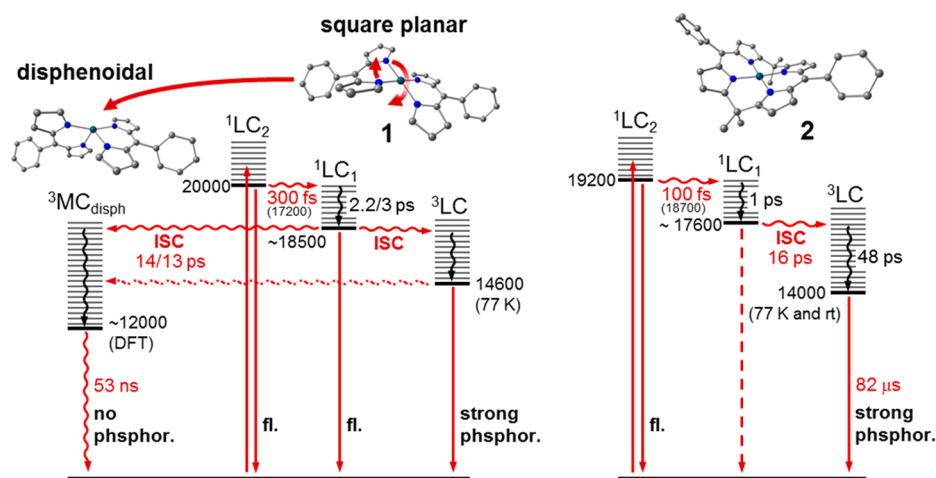


**Figure 8.** State diagram of **1** and **2**. The energies ( $\text{cm}^{-1}$ ) of states were estimated by the intersection of a tangent at the low (high) energy flank of the corresponding absorption (emission) band with the energy axis. The corresponding excited state structures are calculated at the DFT level. The given lifetimes refer to states but approximate inverted rates if one assumes that the assigned process dominates. If two lifetimes are given, the first refers to the TA measurement, the second to the FLUC measurement. Energies in round brackets are emission energies upconverted in the FLUC measurements. The dotted wavy arrow indicates a process at rt which was not observed but also cannot be excluded from our experiments (see main text for details).

$^1\text{LC}_1$  state. A component with  $\tau = 3$  ps in the FLUC decay indicates vibrational relaxation within the  $^1\text{LC}_1$  state. This is supported by two very similar EADS in the deconvolution of the TA spectra (see Figure 3b). Finally, ISC to the lowest lying triplet state occurs with  $\tau = 13$  ps. This change of electronic structure is also visible in the TA spectra by the EADS with  $\tau = 14$  ps which, in contrast to the  $^1\text{LC}$  states, also shows a pronounced ESA, see Figure 4a. The fact that we observe fluorescence from the  $^1\text{LC}_1$  state which, according to exciton coupling theory, should be a dark state, is probably caused by structural flexibility of **1** which disturbs the  $C_1$  symmetry by an asymmetric vibration and makes fluorescence from the  $^1\text{LC}_1$  state partially allowed.

In fluid solution, we expect that the lowest energy triplet state of **1** adopts disphenoidal geometry as supported by the DFT calculations. This state has a rather short lifetime (53 ns), as was proved by nanosecond TA spectroscopy (see Figure 5c), which is typical of states with pronounced  $^3\text{MC}$  character. In agreement with our observations, such a  $^3\text{MC}$  state should be nonemissive.<sup>39</sup> However, complex **1** in frozen MeTHF matrix shows a strong, structured emission, in agreement with phosphorescence from a  $^3\text{LC}$  state which cannot undergo structural reorganization into the  $^3\text{MC}$  state because of the rigid matrix (see Figure 2b). At this point, we stress that we cannot exclude that even at rt a  $^3\text{LC}$  is slowly populated by ISC from the  $^1\text{LC}_1$  state and then relaxes quickly to the  $^3\text{MC}$  state because, if this scenario applies, the intermediate concentration of  $^3\text{LC}$  would be too low to be detectable.

Complex **2** cannot undergo such structural reorganization as **1** because the relative orientation of dipyrin subunits and thereby the coordination sphere of the Pd atom is fixed by the two dimethylmethylene bridges. On the other hand, the ground state structure is different from that of **1**, as was discussed above. Excitation of the strongly allowed  $^1\text{LC}_2$  state is followed by IC to the dark  $^1\text{LC}_1$  state with  $1/\tau = (0.1 \text{ ps})^{-1}$  as seen in the FLUC experiment (see Figure 6b). A weak component with  $\tau = 1$  ps may indicate vibrational relaxation within the  $^1\text{LC}_1$  state. This state is so weakly fluorescent that we were unable to get reasonable data by FLUC spectroscopy to characterize the

ISC process to the  $^3\text{LC}$  state. However, from TA spectroscopy, the EADS with  $\tau = 16$  ps shows a similar spectral change to the following EADS as in the case of complex **1**. Thus, it is likely that this process refers to ISC with  $1/\tau = (16 \text{ ps})^{-1}$ . This change of electronic structure goes along with the rise of a strong ESA in the TA spectra as is also visible in the following EADS with  $\tau = 48$  ps (see Figure 4b). We assign this time constant to a slow vibrational relaxation within the  $^3\text{LC}$  state. As shown by nanosecond TA spectroscopy, this state has a lifetime of 82  $\mu\text{s}$  (see Figure 5d) and is also emissive both at rt in fluid MeCN and in frozen MeTHF (see Figure 2b) because it cannot rearrange to a disphenoidal structure as in case of **1**. Nanosecond TA measurements in fluid THF and toluene gave almost identical results with somewhat longer lifetimes (see Figures S3 and S4 in the Supporting Information), ruling out the participation of any interligand CT states in the relaxation pathway.<sup>10</sup>

In conclusion, the photophysics of complexes **1** and **2** is governed by a fast ISC process from LC states to triplet states ( $1/\tau \approx (13 \text{ ps})^{-1} - (16 \text{ ps})^{-1}$ ). This ISC rate constant is comparable to those of other Pd(II) complexes.<sup>40</sup> While the bis-dipyrin complex **1** can undergo structural reorganization toward a nonemissive  $^3\text{MC}$  state, this is impeded by the structurally more rigid bridged ligand in complex **2** which therefore shows significant NIR phosphorescence even in fluid solution at rt.<sup>41,42</sup>

## ■ ASSOCIATED CONTENT

### Supporting Information

The Supporting Information is available free of charge on the ACS Publications website at DOI: 10.1021/acs.inorgchem.8b00974.

Synthesis, analytical methods, steady state electronic spectra, transient absorption spectra, X-ray crystallographic data, and computational results (PDF)

### Accession Codes

CCDC 1835934–1835935 contain the supplementary crystallographic data for this paper. These data can be obtained free of charge via [www.ccdc.cam.ac.uk/data\\_request/cif](http://www.ccdc.cam.ac.uk/data_request/cif), by emailing

data\_request@ccdc.cam.ac.uk, or by contacting The Cambridge Crystallographic Data Centre, 12 Union Road, Cambridge CB2 1EZ, UK; fax: +44 1223 336033.

## AUTHOR INFORMATION

### Corresponding Author

\*E-mail: christoph.lambert@uni-wuerzburg.de.

### ORCID

Frank Würthner: 0000-0001-7245-0471

Christoph Lambert: 0000-0002-9652-9165

### Notes

The authors declare no competing financial interest.

## ACKNOWLEDGMENTS

We thank the Deutsche Forschungsgemeinschaft for support of this work in the GRK 2112 and the Bavarian Ministry of Education, Culture, Research, and the Fine Arts for Support within the Solar Technologies Go Hybrid program.

## REFERENCES

- (1) Arbeloa, T. L.; Arbeloa, F. L.; Arbeloa, I. L.; Garcia-Moreno, I.; Costela, A.; Sastre, R.; Amat-Guerri, F. Correlations between photophysics and lasing properties of dipyrromethene-BF<sub>2</sub> dyes in solution. *Chem. Phys. Lett.* **1999**, *299*, 315–321.
- (2) Loudet, A.; Burgess, K. BODIPY dyes and their derivatives: Syntheses and spectroscopic properties. *Chem. Rev.* **2007**, *107*, 4891–4932.
- (3) Ulrich, G.; Zissel, R.; Harriman, A. The chemistry of fluorescent bодipy dyes: Versatility unsurpassed. *Angew. Chem., Int. Ed.* **2008**, *47*, 1184–1201.
- (4) Boens, N.; Leen, V.; Dehaen, W. Fluorescent indicators based on BODIPY. *Chem. Soc. Rev.* **2012**, *41*, 1130–1172.
- (5) Wood, T. E.; Thompson, A. Advances in the chemistry of dipyririns and their complexes. *Chem. Rev.* **2007**, *107*, 1831–1861.
- (6) Baudron, S. A. Luminescent dipyririn based metal complexes. *Dalton Trans.* **2013**, *42*, 7498–7509.
- (7) Antina, E. V.; Romyantsev, E. V.; Dudina, N. A.; Marfin, Y. S.; Antina, L. A. Actual aspects of the chemistry of dipyririn dyes and prospects for their application in molecular sensorics. *Russ. J. Gen. Chem.* **2016**, *86*, 2209–2225.
- (8) Re, N.; Bonomo, L.; Da Silva, C.; Solari, E.; Scopelliti, R.; Floriani, C. A structural and theoretical analysis of transition metalporphodimethenes and their relationship with metalporphyrins. *Chem. - Eur. J.* **2001**, *7*, 2536–2546.
- (9) Sazanovich, I. V.; Kirmaier, C.; Hindin, E.; Yu, L. H.; Bocian, D. F.; Lindsey, J. S.; Holten, D. Structural control of the excited-state dynamics of bis(dipyririnato)zinc complexes: Self-assembling chromophores for light-harvesting architectures. *J. Am. Chem. Soc.* **2004**, *126*, 2664–2665.
- (10) Trinh, C.; Kirlikovali, K.; Das, S.; Ener, M. E.; Gray, H. B.; Djurovich, P.; Bradforth, S. E.; Thompson, M. E. Symmetry-Breaking Charge Transfer of Visible Light Absorbing Systems: Zinc Dipyririns. *J. Phys. Chem. C* **2014**, *118*, 21834–21845.
- (11) Thoi, V. S.; Stork, J. R.; Magde, D.; Cohen, S. M. Luminescent dipyririnato complexes of trivalent group 13 metal ions. *Inorg. Chem.* **2006**, *45*, 10688–10697.
- (12) Tsuchiya, M.; Sakamoto, R.; Shimada, M.; Yamanoi, Y.; Hattori, Y.; Sugimoto, K.; Nishibori, E.; Nishihara, H. Bis(dipyririnato)zinc(II) Complexes: Emission in the Solid State. *Inorg. Chem.* **2016**, *55*, 5732–5734.
- (13) Kusaka, S.; Sakamoto, R.; Kitagawa, Y.; Okumura, M.; Nishihara, H. An Extremely Bright Heteroleptic Bis(dipyririnato)zinc(II) Complex. *Chem. - Asian J.* **2012**, *7*, 907–910.
- (14) Kusaka, S.; Sakamoto, R.; Nishihara, H. Luminescent Heteroleptic Tris(dipyririnato)indium(III) Complexes. *Inorg. Chem.* **2014**, *53*, 3275–3277.
- (15) Sakamoto, R.; Iwashima, T.; Kogel, J. F.; Kusaka, S.; Tsuchiya, M.; Kitagawa, Y.; Nishihara, H. Dissymmetric Bis(dipyririnato)zinc(II) Complexes: Rich Variety and Bright Red to Near-Infrared Luminescence with a Large Pseudo-Stokes Shift. *J. Am. Chem. Soc.* **2016**, *138*, 5666–5677.
- (16) Sakamoto, R.; Iwashima, T.; Tsuchiya, M.; Toyoda, R.; Matsuoka, R.; Kogel, J. F.; Kusaka, S.; Hoshiko, K.; Yagi, T.; Nagayama, T.; Nishihara, H. New aspects in bis and tris(dipyririnato)-metal complexes: bright luminescence, self-assembled nanoarchitectures, and materials applications. *J. Mater. Chem. A* **2015**, *3*, 15357–15371.
- (17) Ramlot, D.; Rebarz, M.; Volker, L.; Ovaere, M.; Beljonne, D.; Dehaen, W.; Van Meervelt, L.; Moucheron, C.; Kirsch-De Mesmaeker, A. An Experimental and Theoretical Approach to the Photophysical Properties of Some Rh and Ir Complexes Incorporating the Dipyrromethene Ligand. *Eur. J. Inorg. Chem.* **2013**, *2013*, 2031–2040.
- (18) Hall, J. D.; McLean, T. M.; Smalley, S. J.; Waterland, M. R.; Telfer, S. G. Chromophoric dipyririn complexes capable of binding to TiO<sub>2</sub>: Synthesis, structure and spectroscopy. *Dalton Trans.* **2010**, *39*, 437–445.
- (19) Das, S.; Gupta, I. Triphenylamine substituted dipyririnato metal complexes: Synthesis, optical and electrochemical studies. *Inorg. Chem. Commun.* **2015**, *60*, 54–60.
- (20) Klein, J. H.; Schmidt, D.; Steiner, U. E.; Lambert, C. Complete Monitoring of Coherent and Incoherent Spin Flip Domains in the Recombination of Charge-Separated States of Donor-Iridium Complex-Acceptor Triads. *J. Am. Chem. Soc.* **2015**, *137*, 11011–11021.
- (21) Hanson, K.; Tamayo, A.; Diev, V. V.; Whited, M. T.; Djurovich, P. I.; Thompson, M. E. Efficient Dipyririn-Centered Phosphorescence at Room Temperature from Bis-Cyclometalated Iridium(III) Dipyririnato Complexes. *Inorg. Chem.* **2010**, *49*, 6077–6084.
- (22) Klein, J. H.; Sunderland, T. L.; Kaufmann, C.; Holzapfel, M.; Schmiedel, A.; Lambert, C. Stepwise versus pseudo-concerted two-electron-transfer in a triarylamine-iridium dipyririn-naphthalene diimide triad. *Phys. Chem. Chem. Phys.* **2013**, *15*, 16024–16030.
- (23) Bronner, C.; Baudron, S. A.; Hosseini, M. W.; Strassert, C. A.; Guenet, A.; De Cola, L. Dipyririn based luminescent cyclometalated palladium and platinum complexes. *Dalton Trans.* **2010**, *39*, 180–184.
- (24) Pomarico, E.; Silatani, M.; Messina, F.; Braem, O.; Cannizzo, A.; Barranoff, E.; Klein, J. H.; Lambert, C.; Chergui, M. Dual Luminescence, Interligand Decay, and Nonradiative Electronic Relaxation of Cyclometalated Iridium Complexes in Solution. *J. Phys. Chem. C* **2016**, *120*, 16459–16469.
- (25) Bronner, C.; Veiga, M.; Guenet, A.; De Cola, L.; Hosseini, M. W.; Strassert, C. A.; Baudron, S. A. Excited State Properties and Energy Transfer within Dipyririn-Based Binuclear Iridium/Platinum Dyads: The Effect of ortho-Methylation on the Spacer. *Chem. - Eur. J.* **2012**, *18*, 4041–4050.
- (26) Lambert, C.; Wagoner, R.; Klein, J. H.; Grelaud, G.; Moos, M.; Schmiedel, A.; Holzapfel, M.; Bruhn, T. A photoinduced mixed-valence state in an organic bis-triarylamine mixed-valence compound with an iridium-metal-bridge. *Chem. Commun.* **2014**, *50*, 11350–11353.
- (27) Muthukumar, K.; Zaidi, S. H. H.; Yu, L. H.; Thamyongkit, P.; Calder, M. E.; Sharada, D. S.; Lindsey, J. S. Synthesis of dipyririn-containing architectures. *J. Porphyrins Phthalocyanines* **2005**, *9*, 745–759.
- (28) Sharada, D. S.; Muresan, A. Z.; Muthukumar, K.; Lindsey, J. S. Direct synthesis of palladium porphyrins from acyldipyrromethanes. *J. Org. Chem.* **2005**, *70*, 3500–3510.
- (29) Sazanovich, I. V.; Balakumar, A.; Muthukumar, K.; Hindin, E.; Kirmaier, C.; Diers, J. R.; Lindsey, J. S.; Bocian, D. F.; Holten, D. Excited-state energy-transfer dynamics of self-assembled imine-linked porphyrin dyads. *Inorg. Chem.* **2003**, *42*, 6616–6628.
- (30) Beziau, A.; Baudron, S. A.; Fluck, A.; Hosseini, M. W. From Sequential to One-Pot Synthesis of Dipyririn Based Grid-Type Mixed Metal Organic Frameworks. *Inorg. Chem.* **2013**, *52*, 14439–14448.
- (31) Senge, M. O. Exercises in molecular gymnastics - bending, stretching and twisting porphyrins. *Chem. Commun.* **2006**, 243–256.

- (32) Telfer, S. G.; McLean, T. M.; Waterland, M. R. Exciton coupling in coordination compounds. *Dalton Trans.* **2011**, *40*, 3097–3108.
- (33) Waterland, M. R.; Telfer, S. G.; McLean, T. M. Controlling molecular excitons with coordination chemistry. *Chem. N. Z.* **2010**, *74*, 15–19.
- (34) Holaday, M. G. D.; Tarafdar, G.; Kumar, A.; Reddy, M. L. P.; Srinivasan, A. Exploring anagostic interactions in 5,15-porphodime-thene metal complexes. *Dalton Trans.* **2014**, *43*, 7699–7703.
- (35) Brückner, C.; Engels, B. Benchmarking singlet and triplet excitation energies of molecular semiconductors for singlet fission: Tuning the amount of HF exchange and adjusting local correlation to obtain accurate functionals for singlet-triplet gaps. *Chem. Phys.* **2017**, *482*, 319–338.
- (36) Yeo, J. S. L.; Vittal, J. J.; Hor, T. S. A. PdCl<sub>2</sub>(dppfO(2)-O, O'): a simple palladium(II) complex with a rare tetrahedral structure. *Chem. Commun.* **1999**, 1477–1478.
- (37) Tsay, C.; Mankad, N. P.; Peters, J. C. Four-Coordinate, Trigonal Pyramidal Pt(II) and Pd(II) Complexes. *J. Am. Chem. Soc.* **2010**, *132*, 13975–13977.
- (38) Frech, C. M.; Shimon, L. J. W.; Milstein, D. Redox-induced collapse and regeneration of a pincer-type complex framework: A nonplanar coordination mode of palladium(II). *Angew. Chem., Int. Ed.* **2005**, *44*, 1709–1711.
- (39) Sauvage, J. P.; Collin, J. P.; Chambron, J. C.; Guillerez, S.; Coudret, C.; Balzani, V.; Barigelletti, F.; Decola, L.; Flamigni, L. Ruthenium(II) and Osmium(II) Bis(terpyridine) Complexes in Covalently-Linked Multicomponent Systems - Synthesis, Electrochemical-Behavior, Absorption-Spectra, and Photochemical and Photophysical Properties. *Chem. Rev.* **1994**, *94*, 993–1019.
- (40) Chow, P.-K.; Cheng, G.; Tong, G. S. M.; Ma, C.; Kwok, W.-M.; Ang, W.-H.; Chung, C. Y.-S.; Yang, C.; Wang, F.; Che, C.-M. Highly luminescent palladium(II) complexes with sub-millisecond blue to green phosphorescent excited states. *Photocatalysis and highly efficient PSF-OLEDs Chemical Science* **2016**, *7*, 6083–6098.
- (41) Schulze, M.; Steffen, A.; Würthner, F. Near-IR Phosphorescent Ruthenium(II) and Iridium(III) Perylene Bisimide Metal Complexes. *Angew. Chem., Int. Ed.* **2015**, *54*, 1570–1573.
- (42) Xiang, H.; Cheng, J.; Ma, X.; Zhou, X.; Chruma, J. J. Near-infrared phosphorescence: materials and applications. *Chem. Soc. Rev.* **2013**, *42*, 6128–6185.